International Journal of
Intelligent Systems and Applications in Engineering

ISSN:2147-6799 www.ijisae.org Original Research Paper

Fusion of CT and MR Liver Images by SURF-Based Registration

Muhammet Fatih Aslan*[1], Akif Durdu[2], Kadir Sabanci[3]

Submitted: 23/09/2019 Accepted : 12/12/2019

Abstract: Medical imaging plays an important role in the diagnosis and treatment of different diseases. Images with more details are obtained by image fusion for more accurate analysis of medical images. In this study, Computed Tomography (CT) and Magnetic Resonance (MR) images of the liver from The Cancer Genome Atlas Liver Hepatocellular Carcinoma (TCGA-LIHC) are fused using different combinations of different wavelet types such as daubechies, coiflet and symlet. To accomplish this task, first the preprocessing steps are completed, and then registration is performed using Speed up Robust Features (SURF). As a result, to measure the quality of the obtained fusion image Peak Signal-to-Noise Ratio (PSNR), Mean Squared Error (MSE), Structural Similarity Index Measurement (SSIM), Mean Structural Similarity (MSSIM) and Feature Similarity Index (FSIM) metrics are used.

Keywords: *Image Fusion, SURF, Wavelet transform*

1. Introduction

Image fusion aims to combine images from different sensors to create a powerful and informative image in image-based decision-making applications. Today, image fusion applications have gained importance due to the development of sensor technology. For successful image fusion, useful information should be effectively extracted and appropriate fusion methods should be used without creating an artefact in the original image. As a result of image fusion, the original image contains richer information. For this reason, they are used in a wide range of areas such as image-based intelligent robotic systems, medical applications, military defense applications and remote sensing. Among these, remote sensing is the most common field of image fusion [1-4].

Applications of imaging technologies in the field of medical diagnosis and analysis are increasing. However, due to technical limitations, the quality of the acquired medical images is generally unsatisfactory. This makes image analysis difficult and may lead to incorrect decisions. Medical image fusion improves the quality of medical images to improve clinical applicability. Because images are digitally evaluated using computer-aided imaging techniques, physicians can make an objective decision in a short time. In addition, information that cannot be noticed by the human eye is revealed. For this, fusion images containing information from more than one image can provide a more precise localization of the disease or abnormality [5-7].

Magnetic Resonance (MR), computed tomography (CT) and ultrasound (US) images are medical images that provide structural information of organs. In addition, medical imaging methods such as Functional Magnetic Resonance (fMR), Single Photon Emission Computed Tomography (SPECT) and Positron Emission Tomography (PET) are available. However, each method gives more information in limited space. It is not possible to obtain complete, comprehensive and accurate information with a single imaging method. For example, MR images reflect soft tissue information, while CT images provide bone tissue and bone structure information. Therefore, combining both information into a single image will provide more accurate and effective results. For example, fusion of CT-MR images can produce an image that identifies soft tissue and bone. Combining PET with CT or MRI provides both anatomical and metabolic information. Fusion of MR-PET images is used to detect brain tumors [8, 9].

There are various methods for performing image fusion, such as Intensity Hue Saturation (IHS), Brovey transform (BT), Principal Component Analysis (PCA), and wavelet analysis. Recent studies mostly involve wavelet-based hybrid methods. Although these hybrid approaches provide more accurate results than standard image fusion methods (IHS, PCA, CT, etc.) and standard wavelet based image fusion methods, they have more computational complexity [10].

In this study, CT and MR images were fused using different wavelet transform types. Prior to wavelet transformation, preprocessing and Speed Up Robust Features (SURF) based registration were performed. Then, the approximate and detail coefficients of both images were obtained by applying wavelet transform. These coefficients are combined according to the desired rule in the prepared Matlab Graphical User Interface (GUI). The similarity of the obtained fusion images to the source images was calculated with PSNR, MSE, SSIM, MSSIM and FSIM metrics.

2. Related Works

Various algorithms have been proposed in the field of medical image fusion in the literature due to their important application areas.Singh, et al. [8] presented a new fusion method for CT and MRI medical images using both Nonsubsampled Shearlet Transform (NSST) and Spiking Neural Network. Ganasala and

[1]*Department of Electrical-Electronic Engineering, Karamanoğlu Mehmetbey University,Karaman,-70100, Turkey,*
ORCID ID : 0000-0001-7549-0137
[2]*Department of Electrical-Electronic Engineering, Konya Technical University,Konya,-42000, Turkey,*
ORCID ID : 0000-0002-5611-2322
[3]*Department of Electrical-Electronic Engineering, Karamanoğlu Mehmetbey University,Karaman,-70100, Turkey,*
ORCID ID : 0000-0003-0238-9606
** Corresponding Author: Email: mfatihaslan@kmu.edu.tr*

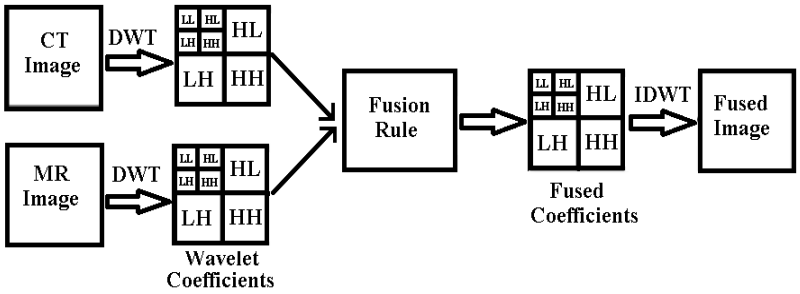

Fig. 1. Structure of wavelet based image fusion

Kumar [11] separated source images using Nonsubsampled Contourlet Transform (NSCT). Maximum entropy of the square of the coefficients and sum-modified Laplacian were used for low frequency and high frequency subband coefficient selection, respectively. The fusion image was then obtained with reverse NCST. Sekhar and Prasad [12] proposed a multiresolution fusion algorithm that combines the features of region and pixel-based fusion. In this study, fusion method was carried out by using wavelet and PCA together. In a different study, Rajkumar, et al. [13] used two fusion techniques: Iterative Neuro-Fuzzy Approach (INFA), Lifting Wavelet Transform-Neuro-Fuzzy Approach (LWT-NFA). Using the proposed techniques, CT and MR images were fused. Finally, Ali, et al. [14] presented a curvelet-based approach for the fusion of MRI and CT images. Since several objects of the medical images have a curved shape, the curvelet transformation has given better results.

3. Wavelet Based Fusion

Image fusion combines information from different images from the same scene. Wavelet is a multiresolution approach suitable for different image resolutions. By using Discrete Wavelet Transform (DWT), the image is decomposed by different kinds of coefficients that protect the image information. The separation results in low-high (LH), high-low (HL), high-high (HH) and low-low (LL) bands. In bands other than LL, edges and lines are more pronounced. In fusion applications, these coefficients from different images are combined appropriately to obtain new coefficients. In this way, the information in the original images is put together appropriately using fusion rules. There are too many fusion rules. The basic rule is to get the maximum, minimum or average of the coefficients. Once the coefficients are combined, the fusion image is obtained by means of the İnverse Discrete Wavelet Transform (IDWT), which preserves the information in the combined coefficients [15-17]. The wavelet-based fusion structure of CT and MR images is shown in Fig. 1.

4. Image Registration

Before fusion of two images, one image is referenced for fusion of the same regions in both images, and the other image is recorded relative to that image. This is called image registration.
In order to achieve the best match with image registration in pixel layer, conversion parameters are obtained between images taken at different times from different angles. Image registration is a key topic for many computer vision technologies, such as image enhancement, tracking, image fusion, 3D reconstruction, and pattern recognition [18]. In this application, SURF [19] matching based registration method was used for fusion of CT and MR images.

5. Application and Results

In this application, The Cancer Genome Atlas Liver Hepatocellular Carcinoma (TCGA-LIHC) dataset [20-22] was used. CT and MR images of the liver in this dataset were fused. Some of the CT and MR images used for the application are shown in Fig. 2 and Fig. 3, respectively. The original version of both image types is not suitable for fusion. For this reason, preprocessing - image registration - fusion steps were performed respectively.

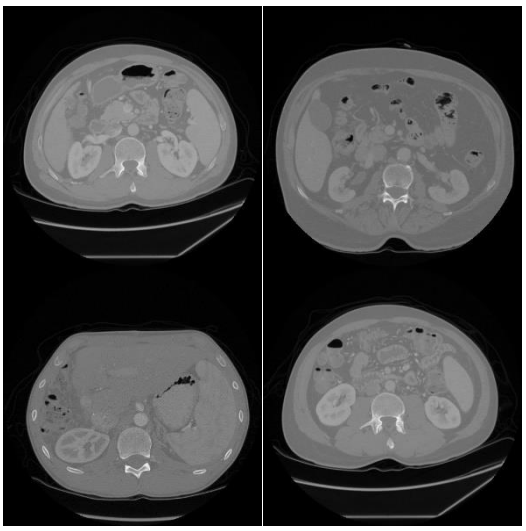

Fig. 2. Some CT images used in application

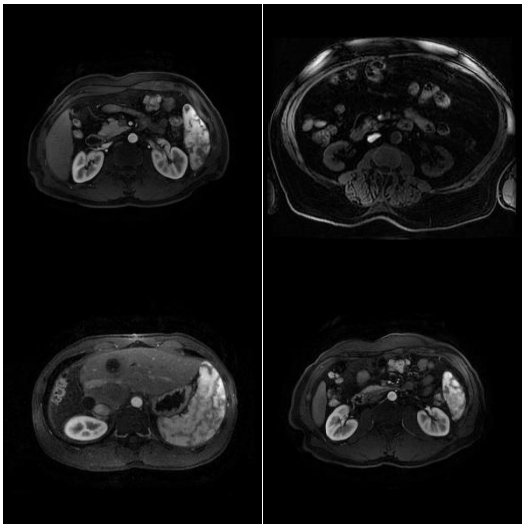

Fig. 3. Some MR images used in application

The preprocessing steps for noisy images of different sizes shown in Fig. 2 and Fig. 3 are shown in Fig. 4. In addition, CT result images obtained as a result of preprocessing steps were added.

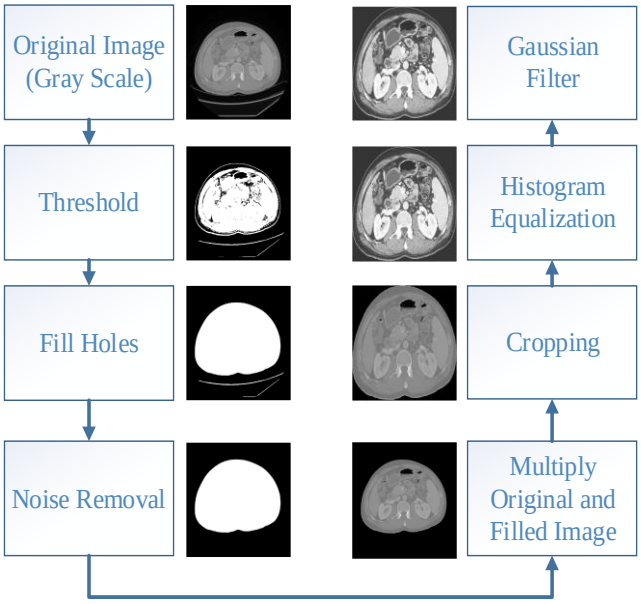

Fig. 4. Preprocessing steps for CT image

In the last step, the cropped, a less noisy, higher contrast image is obtained. These steps are performed for both CT and MR images. MR and CT images to be fused after the preprocessing steps are resized to the same size. However, for successful fusion, the same regions in the images must overlap. When the Fig. 5 is examined, it can be seen that the same organs are not fully overlapping. This can be seen more clearly in Fig. 6. Gray areas in the overlapping image correspond to areas with similar densities. Magenta and green areas indicate where one image is brighter than the other.

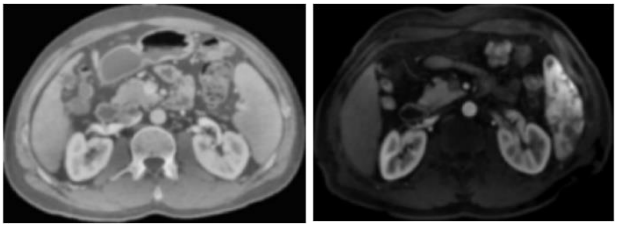

Fig. 5. CT and MR images after preprocessing steps

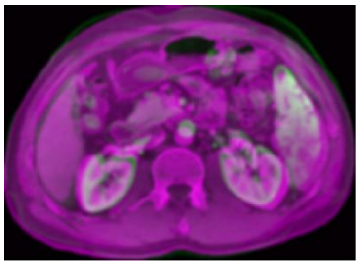

Fig. 6. Overlapped CT and MR images

In this study, in order to overlap the different localizations of the same regions shown in Fig. 6, i.e. image registration, SURF method was applied. Image matching is performed using SURF. This way, similar points in both images are matched. The transformation matrix is then applied according to these keypoints. The keypoints detected by SURF are shown in Fig. 7. The image registration result at the end of the transformation according to the keypoints in Fig. 7 is shown in Fig. 8.

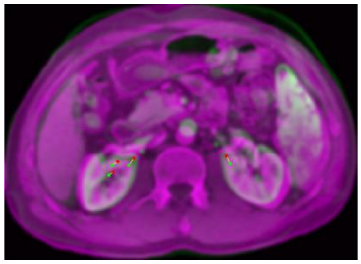

Fig. 7. Matching CT and MR images using SURF

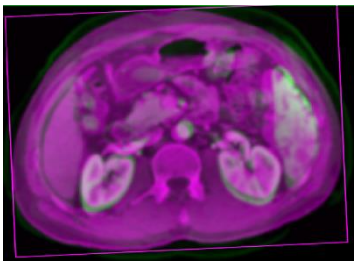

Fig. 8. Image registration

After the image registration, as shown in Figure 8, it is ensured that the same regions in both images overlap more accurately. The fusion can now be performed using the transformed CT image. In this experiment, the CT image was registered according to the MR image. The resulting new CT image is shown in Fig. 9. This new image obtained as a result of the image registration process also needs preprocessing. Therefore, after preprocessing on this image, fusion operations were applied. The GUI developed for this application can be seen in Fig. 10. In the fusion step, different wavelet types for decomposition and different methods for fusion rule can be optionally set in the GUI. The wavelet types used are Daubechies (db), Coiflets (coif) and Symlets (sym).

Fig. 9. CT image after image registration

Maximum, minimum and average methods were used for fusion rule. The fusion image obtained as a result of these various combinations was compared with both CT and MR image using PSNR, MSE, SSIM, MSSIM and FSIM metrics. The results are shown in Table 1 and Table 2. Wavelet type and fusion rule inputs were selected according to the best values in Table 1. First, the best wavelet type and decomposition level were determined for the 'max' - 'max' fusion rule. Since the best results for 'sym' and '1' were obtained, the fusion rule values were subsequently modified. As a result of the comparison with CT image, the best values were obtained for 'sym', '1', 'max', 'max'. Using the input values in Table 1, the fusion image and the MR image were compared and the results are shown in Table 2.

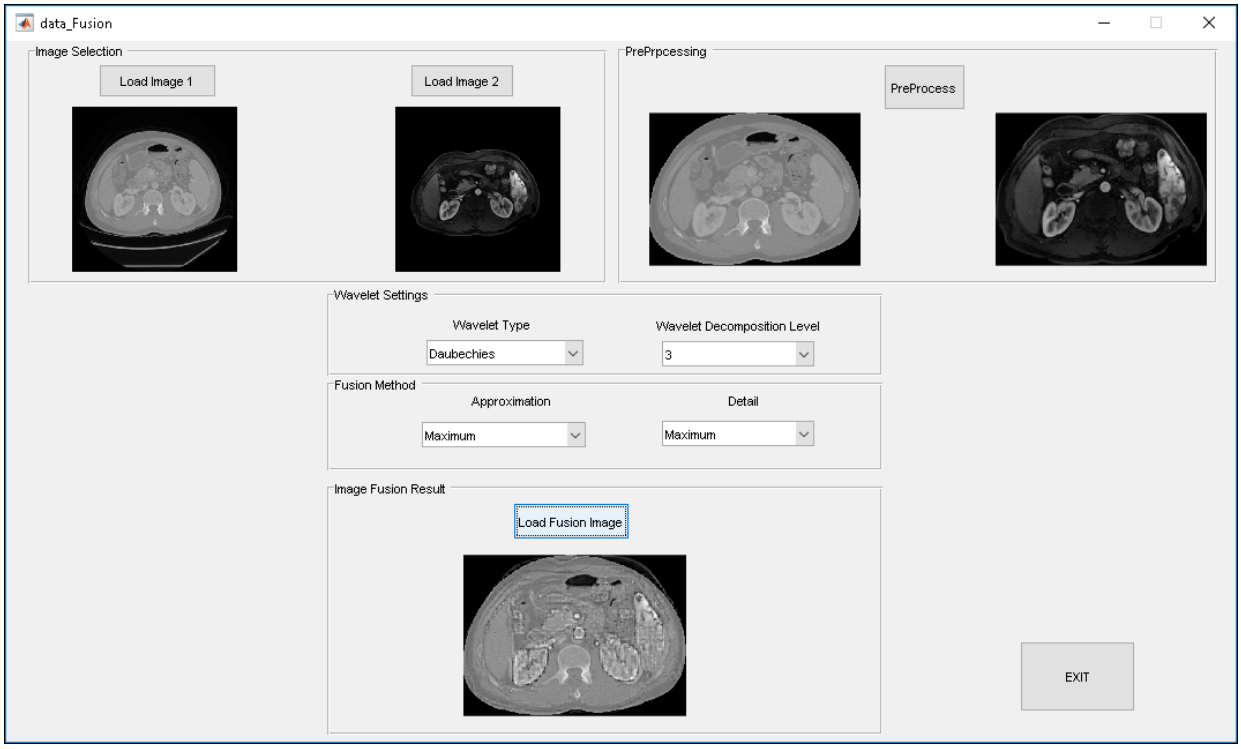

Fig. 10. GUI designed for application

Table 1. Values obtained by comparison of CT and fusion image

Wavelet Type	Decomp. Level	Fusion Rule of Approx. Coef.	Fusion Rule of Detail Coef.	MSE	PSNR	SSIM	MSSIM	FSIM
'db'	'1'	'max'	'max'	68.742	29.759	0.90464	0.91888	0.94436
'db'	'2'	'max'	'max'	81.317	29.029	0.83961	0.84934	0.93212
'db'	'3'	'max'	'max'	118.13	27.407	0.78232	0.79422	0.88547
'db'	'4'	'max'	'max'	198.51	25.153	0.75929	0.78799	0.83593
'coif'	'1'	'max'	'max'	65.609	29.961	0.93512	0.94981	0.94551
'coif'	'2'	'max'	'max'	69.208	29.729	0.89563	0.91324	0.94106
'coif'	'3'	'max'	'max'	94.108	28.395	0.82771	0.84527	0.88961
'coif'	'4'	'max'	'max'	157.31	26.163	0.78953	0.81001	0.83828
'sym'	**'1'**	**'max'**	**'max'**	**65.592**	**29.962**	**0.9348**	**0.94947**	**0.94549**
'sym'	'2'	'max'	'max'	69.768	29.694	0.89456	0.90931	0.94079
'sym'	'3'	'max'	'max'	97.05	28.261	0.82524	0.84291	0.88813
'sym'	'4'	'max'	'max'	160.49	26.076	0.78719	0.81543	0.83731
'sym'	'1'	'max'	'min'	80.381	29.079	0.92702	0.94354	0.94476
'sym'	'1'	'max'	'mean'	68.937	29.746	0.93614	0.9511	0.94536
'sym'	'1'	'min'	'max'	8581.1	8.7954	0.45415	0.44481	0.67025
'sym'	'1'	'min'	'min'	8610.3	8.7806	0.4452	0.4395	0.66453
'sym'	'1'	'min'	'mean'	8593.6	8.789	0.45141	0.4434	0.6675
'sym'	'1'	'mean'	'max'	2165	14.776	0.7858	0.79528	0.82221
'sym'	'1'	'mean'	'min'	2180.8	14.745	0.77401	0.78598	0.82211
'sym'	'1'	'mean'	'mean'	2168.4	14.769	0.78536	0.79547	0.82279

Table 2. Values obtained by comparison of MR and fusion image

Wavelet Type	*Decomp. Level*	*Fusion Rule of Approx. Coef.*	*Fusion Rule of Detail Coef.*	*MSE*	*PSNR*	*SSIM*	MSSIM	FSIM
'db'	'1'	'max'	'max'	8629.7	8.7708	0.44608	0.43954	0.6663
'db'	'2'	'max'	'max'	8602.5	8.7846	0.44943	0.44458	0.67476
'db'	'3'	'max'	'max'	8560.1	8.8060	0.45745	0.46181	0.69881
'db'	'4'	'max'	'max'	8472.3	8.8508	0.46569	0.48737	0.70982
'coif'	'1'	'max'	'max'	8611	8.7803	0.445	0.43773	0.66506
'coif'	'2'	'max'	'max'	8607.3	8.7821	0.44871	0.44112	0.6684
'coif'	'3'	'max'	'max'	8582.1	8.7948	0.46183	0.46177	0.6873
'coif'	'4'	'max'	'max'	8516.1	8.8284	0.46803	0.48221	0.69028
'sym'	'1'	'max'	'max'	8611	8.7803	0.44502	0.43847	0.66514
'sym'	'2'	'max'	'max'	8606.9	8.7824	0.44829	0.44456	0.66784
'sym'	'3'	'max'	'max'	8578.9	8.7965	0.4618	0.45339	0.68759
'sym'	'4'	'max'	'max'	8512.8	8.8301	0.46794	0.47791	0.69179
'sym'	'1'	'max'	'min'	8595.5	8.7881	0.44553	0.43768	0.66443
'sym'	'1'	'max'	'mean'	8599.3	8.7862	0.44672	0.43933	0.66484
'sym'	'1'	'min'	'max'	73.512	29.467	0.89938	0.92414	0.91682
'sym'	**'1'**	**'min'**	**'min'**	**64.224**	**30.054**	**0.93146**	**0.94242**	**0.92078**
'sym'	'1'	'min'	'mean'	66.913	29.876	0.91627	0.93769	0.91931
'sym'	'1'	'mean'	'max'	2179.9	14.746	0.63133	0.62961	0.78436
'sym'	'1'	'mean'	'min'	2165.7	14.775	0.63648	0.63336	0.78415
'sym'	'1'	'mean'	'mean'	2170.2	14.766	0.63586	0.63294	0.78354

6. Conclusion

In this study, fusion of CT and MR images was performed. First, both images were preprocessed and the resulting CT image was registered according to the MR image. For this purpose, the same points in both images were determined using SURF keypoints. Accordingly, a new CT image was obtained for a more accurate overlap with the MR image. After preprocessing steps on this image, both images were fused using different wavelet families and different fusion rules. Using the GUI designed for this, MSE, PSNR, SSIM, MSSIM and FSIM values of different parameter inputs were obtained. When the results are examined, the fusion image is more similar to the original CT image if the approximate and detail coefficients are selected as ‘max’. If the approximate and detail coefficients are selected as ‘min’, the fusion image is more similar to the original MR image. The best wavelet family for this is the symlet, and the decomposition level is 1.

References

[1] J. Ma, Y. Ma, and C. Li, "Infrared and visible image fusion methods and applications: A survey," *Information Fusion*, vol. 45, pp. 153-178, 2019.

[2] G. Piella, "A general framework for multiresolution image fusion: from pixels to regions," *Information fusion*, vol. 4, no. 4, pp. 259-280, 2003.

[3] J. Wang, J. Peng, X. Feng, G. He, and J. Fan, "Fusion method for infrared and visible images by using non-negative sparse representation," *Infrared Physics & Technology*, vol. 67, pp. 477-489, 2014.

[4] Y. Liu, X. Chen, Z. Wang, Z. J. Wang, R. K. Ward, and X. Wang, "Deep learning for pixel-level image fusion: Recent advances and future prospects," *Information Fusion*, vol. 42, pp. 158-173, 2018.

[5] A. P. James and B. V. Dasarathy, "Medical image fusion: A survey of the state of the art," *Information Fusion*, vol. 19, pp. 4-19, 2014.

[6] L. Shuaiqi, Z. Jie, and S. Mingzhu, "Medical image fusion based on rolling guidance filter and spiking cortical model," *Computational and Mathematical Methods in Medicine*, vol. 2015, 2015.

[7] S. Li, H. Yin, and L. Fang, "Group-sparse representation with dictionary learning for medical image denoising and fusion," *IEEEansactions on biomedical engineering*, vol. 59, no. 12, pp. 3450-3459, 2012.

[8] S. Singh, D. Gupta, R. Anand, and V. Kumar, "Nonsubsampled shearlet based CT and MR medical image fusion using biologically inspired spiking neural network," *Biomedical Signal Processing and Control*, vol. 18, pp. 91-101, 2015.

[9] A. Galande and R. Patil, "The art of medical image fusion: A survey," in *2013 International Conference on Advances in Computing, Communications and Informatics (ICACCI)*, 2013, pp. 400-405: IEEE.

[10] R. Gharbia, A. T. Azar, A. E. Baz, and A. E. Hassanien, "Image fusion techniques in remote sensing," *arXiv preprint arXiv:1403.5473*, 2014.

[11] P. Ganasala and V. Kumar, "CT and MR image fusion scheme in nonsubsampled contourlet transform domain," *Journal of digital imaging*, vol. 27, no. 3, pp. 407-418, 2014.

[12] A. S. Sekhar and M. N. G. Prasad, "A novel approach of image fusion on MR and CT images using wavelet transforms," in *2011 3rd International Conference on Electronics Computer Technology*, 2011, vol. 4, pp. 172-176.

[13] S. Rajkumar, P. Bardhan, S. K. Akkireddy, and C. Munshi, "CT and MRI image fusion based on Wavelet Transform and Neuro-Fuzzy concepts with quantitative analysis," in *2014 International Conference on Electronics and Communication Systems (ICECS)*, 2014, pp. 1-6.

[14] F. Ali, I. El-Dokany, A. Saad, and F. E.-S. Abd El-Samie, "Curvelet fusion of MR and CT images," *Progress in Electromagnetics Research*, vol. 3, pp. 215-224, 2008.

[15] G. Pajares and J. M. De La Cruz, "A wavelet-based image fusion tutorial," *Pattern recognition*, vol. 37, no. 9, pp. 1855-1872, 2004.

[16] L. Chiorean and M.-F. Vaida, "Medical image fusion based on discrete wavelet transform using Java technology," in *Proceedings of the ITI 2009 31st International Conference on Information Technology Interfaces*, 2009, pp. 55-60: IEEE.

[17] M. Ceylan and A. E. Canbilen, "Performance Comparison of Tetrolet Transform and Wavelet-Based Transforms for Medical Image Denoising," *International Journal of Intelligent Systems and Applications in Engineering*, vol. 5, no. 4, pp. 222-231, 2017.

[18] Y. Lu, K. Gao, T. Zhang, and T. Xu, "A novel image registration approach via combining local features and geometric invariants," *PloS one*, vol. 13, no. 1, p. e0190383, 2018.

[19] H. Bay, T. Tuytelaars, and L. Van Gool, "Surf: Speeded up robust features," in *European conference on computer vision*, 2006, pp. 404-417: Springer.
[20] B. Erickson *et al.*, "Radiology Data from The Cancer Genome Atlas Liver Hepatocellular Carcinoma [TCGA-LIHC] collectionThe," *Cancer Imaging Archive*, 2016.
[21] K. Clark *et al.*, "The Cancer Imaging Archive (TCIA): maintaining and operating a public information repository," *Journal of digital imaging*, vol. 26, no. 6, pp. 1045-1057, 2013.
[22] TCIA. *Cancer Imaging Archive*. Available: https://www.cancerimagingarchive.net/